Impact of murine intestinal apolipoprotein A-IV expression on regional lipid absorption, gene expression, and growth

Trang Simon,* Victoria R. Cook,* Anuradha Rao,* and Richard B. Weinberg[1,*,†]

Departments of Internal Medicine* and Physiology and Pharmacology,[†] Wake Forest University School of Medicine, Winston-Salem, NC

Abstract **Apolipoprotein A-IV (apoA-IV) is synthesized by intestinal enterocytes during lipid absorption and secreted into lymph on the surface of nascent chylomicrons. A compelling body of evidence supports a central role of apoA-IV in facilitating intestinal lipid absorption and in regulating satiety, yet a longstanding conundrum is that no abnormalities in fat absorption, feeding behavior, or weight gain were observed in chow-fed apoA-IV knockout (A4KO) mice. Herein we reevaluated the impact of apoA-IV expression in C57BL6 and A4KO mice fed a high-fat diet. Fat balance and lymph cannulation studies found no effect of intestinal apoA-IV gene expression on the efficiency of fatty acid absorption, but gut sac transport studies revealed that apoA-IV differentially modulates lipid transport and the number and size of secreted triglyceride-rich lipoproteins in different anatomic regions of the small bowel. ApoA-IV gene deletion increased expression of other genes involved in chylomicron assembly, impaired the ability of A4KO mice to gain weight and increase adipose tissue mass, and increased the distal gut hormone response to a high-fat diet. Together these findings suggest that apoA-IV may play a unique role in integrating feeding behavior, intestinal lipid absorption, and energy storage.**—Simon, T., V. R. Cook, A. Rao, and R. B. Weinberg. **Impact of murine intestinal apolipoprotein A-IV expression on regional lipid absorption, gene expression, and growth.** ***J. Lipid Res.*** **2011.** 52: **1984–1994.**

Supplementary key words diet • fat balance • olestra • gut sacs • lipoproteins • energy balance • satiety

Apolipoprotein A-IV (apoA-IV), the largest member of the exchangeable apolipoprotein family (1), is synthesized by intestinal enterocytes during lipid absorption and secreted into mesenteric lymph on the surface of nascent chylomicrons (2, 3). Since its first description in 1974 (4), a broad spectrum of physiologic functions has been proposed for apoA-IV (5, 6). Some of these, such as activating lecithin-cholesterol acyltransferase (7), lipoprotein lipase (8), and cholesterol-ester transfer protein (9) and mediating tissue cholesterol efflux and reverse cholesterol transport (10), are not unique to apoA-IV and are likely the consequence of structural features shared with the other exchangeable apolipoproteins (1). Other functions, such as serving as a lipid antioxidant (11) and suppressing inflammation (12), are novel. Nonetheless, evolutionary, biophysical, and physiological considerations together suggest that the primary biological role of apoA-IV is the regulation of dietary lipid absorption.

Comparative sequence analysis suggests that apoA-IV originated by duplication of the apoA-I gene ~300 million years ago (1), coincident with the divergence of mammals from their reptile/avian ancestors (13). Thus, apoA-IV may have evolved as part of the mammalian lipid absorption paradigm, in which large chylomicrons are secreted into lymph, rather than directly into plasma (14). Indeed, considerable evidence supports a role of apoA-IV in chylomicron assembly: *i*) intestinal apoA-IV synthesis increases up to 5-fold during absorption of long-chain fatty acids (15, 16), which requires chylomicron assembly, but not during absorption of short-chain fatty acids (17), which does not; *ii*) intestinal apoA-IV synthesis is simultaneously inhibited when chylomicron secretion is blocked by the surfactant PL-81 (18); *iii*) within the enterocyte, apoA-IV colocalizes with apoB in pre-Golgi secretory transport vesicles (19); *iv*) the dynamic interfacial properties of apoA-IV are ideally suited to stabilizing expanding lipid interfaces (20); *v*) plasma apoA-IV levels rise after a fatty meal (2) and are depressed in intestinal disorders in which lipid absorption is impaired (21); and *vi*) tetracycline (TET)-regulated apoA-IV expression in IPEC-1 intestinal cells

This work was supported by National Institutes of Health/National Heart, Lung, and Blood Institute Grant HL-30897. Its contents are solely the responsibility of the authors and do not necessarily represent the official views of the National Institutes of Health.

Manuscript received 20 May 2011 and in revised form 25 July 2011.

Published, JLR Papers in Press, August 12, 2011
DOI 10.1194/jlr.M017418

Abbreviations: A4KO, apoA-IV knockout; BA, behenic acid; DGAT2, diacylglycerol-acyltransferase-2; FABP2, fatty acid binding protein-2; GLP-1, glucagon-like peptide-1; MTP, microsomal triglyceride transfer protein; PYY, peptide YY; TET, tetracycline; TG, triglyceride.

[1]To whom correspondence should be addressed.
e-mail: weinberg@wfubmc.edu

increases transcellular lipid transport by enabling secretion of larger triglyceride (TG)-rich lipoproteins (22).

As the investigation of the function of apoA-IV in lipid absorption has proceeded, Tso et al. have generated a significant body of work establishing that apoA-IV also plays a role in the complex neuroendocrine system that regulates satiety and appetite (23). In an elegant series of studies, they showed that apoA-IV acts both peripherally via the cholecystokinin (CCK) receptor and vagal afferents (24) and centrally in the hypothalamus (25) to modulate short-term feeding behavior and gastric emptying. Interestingly, intestinal apoA-IV synthesis is inhibited by the potent satiety adipokine leptin (26) but is upregulated by the distal gut satiety hormone peptide YY (PYY) (27). Together these findings suggest that apoA-IV may play a unique role in integrating feeding behavior and intestinal lipid absorption.

Notwithstanding this compelling body of evidence supporting a central role of apoA-IV in intestinal lipid absorption and appetite regulation, a longstanding conundrum is that no abnormalities in fat absorption, feeding behavior, or weight gain were observed in chow-fed human apoA-IV transgenic (28) or apoA-IV knockout (A4KO) mice (29). The failure to observe a phenotype in these animals could be simply methodological; a consequence of the functional redundancy of the small intestine that masks subtle effects of apoA-IV gene deletion or overexpression on TG absorption; or due to compensatory changes in the systems regulating these important metabolic processes. Alternatively, the physiological impact of apoA-IV might be manifested only under specific dietary conditions.

Herein we have revaluated the impact of murine apoA-IV expression on intestinal lipid absorption, in both intact animals and at the suborgan level, and its effect on food consumption and weight gain in the setting of a high-fat diet. Our findings reveal that although intestinal apoA-IV expression has no impact on total dietary fat absorption when measured by fat balance methods, it does differentially modulate TG transport and the number and size of secreted TG-rich lipoproteins when examined regionally along the length of the small bowel. Moreover, we observed that deletion of the apoA-IV gene increases the expression of other key genes involved in chylomicron assembly and dietary lipid absorption, and impairs the ability of A4KO mice to gain weight and increase adipose tissue mass on a high-fat diet.

EXPERIMENTAL PROCEDURES

Lipids

Egg phosphatidylcholine (EPC), monoolein, oleic acid (Sigma Aldrich, St. Louis, MO), and [^{3}H]oleic acid and [^{14}C]carboxy inulin (PerkinElmer, Boston, MA) were stored under nitrogen at −20°C. For the gut sac experiments, mixtures of oleic acid, monoolein, [^{3}H]oleic acid, EPC, sodium taurocholate, and sodium taurodeoxycholate (30) (Sigma Aldrich) in DMEM media (Invitrogen, Grand Island, NY) were sonicated for 3 min at high power with 15 s pauses to yield mixed micelles with the following final concentrations: 0.45 mM oleic acid, 0.26 mM monoolein, 0.40 mM sodium taurocholate, and 0.54 mM sodium taurodeoxycholate, with a fatty acid/bile salt ratio similar to that of human postprandial mixed micelles (31). Mean specific activity of the labeled micelles was 2.31 ± 0.04 μCi/μmol oleate (n = 35). For lymph cannulation experiments, mixtures of oleic acid, EPC, and sodium taurocholate in PBS buffer were sonicated for 5 min at high power with 30 s pauses to yield mixed micelles with final concentrations of 16 mM oleic acid, 3 mM EPC, and 54 mM taurocholate.

Animals

ApoA-IV knockout mice (29) were extensively backcrossed onto a C57BL6 background. C57BL6 mice were obtained commercially (Charles River, Wilmington, MA). Unless otherwise noted, mice were housed in groups, maintained on a 12 h light-dark cycle, and provided ad libitum access to water and commercial rodent chow (ProLab RMH 3000, PMI Nutrition, Richmond, IN) that provided 26% of calories from protein, 60% from carbohydrate, 14% from fat, and 3.2 Kcal/g. Animal welfare was continuously monitored by an on-site veterinarian. All animal protocols were reviewed and approved by the Wake Forest University School of Medicine Institutional Animal Care and Use Committee.

Dietary fatty acid absorption

Dietary fatty acid (FA) absorption was measured using the Olestra® method (32), in which sucrose polybehenate serves as a nonabsorbable marker, thereby obviating the need to measure total daily dietary intake or fecal output. For these studies, C57BL6 and A4KO mice (n = 5 for each group) were housed individually in cages with wire mesh floors and fed a custom-made synthetic diet that provided 15% of calories from protein, provided by casein; 35% of calories from carbohydrate, provided by sucrose (17.5% by weight) and dextrin (22.8% by weight); 50% of calories from fat (14.5% saturated, 9.7% monounsaturated, and 25.8% polyunsaturated), provided by a mixture of flaxseed, borage, fish, and DHASCO (Martek, Columbia, MD) oils; and 4% sucrose polybehenic acid (Procter and Gamble, Cincinnati, OH). After the animals had been on the diet for two days, fecal pellets from each animal were collected every morning for the next three days, weighed, lyophilized, and stored at −70°C until batch analysis. Weighed samples of the synthetic diet and feces were saponified with methanolic NaOH, extracted with hexane, converted to methyl esters, and analyzed by gas chromatography (33) to quantitate behenic acid (BA, C22:0) and saturated (14:0, 16:0, 18:0), monounsaturated (C18:1), and polyunsaturated (18:1, 18:2, 18:3ω3, 20:5ω3, 22:6ω3) fatty acids. The coefficient of absorption for each FA was computed as $\{1 - (FA/BA)_{feces} / (FA/BA)_{diet}\} \times 100$.

Lymph duct cannulation

Animals were maintained on chow and fasted for 12 h. At 1 h before surgery, the animals were gavaged with 25 μl of sunflower oil to facilitate identification of the thoracic duct. General anesthesia was induced with ketoprofen and isoflurane, and the cysterna chyli was exposed via a left posterior-lateral incision (34). A 0.64 mm ID silastic cannula was inserted into the thoracic duct through a small incision, a second silastic cannula was threaded through the pylorus into the duodenum via an incision in the fundus of the stomach, and the cannulas were fixed in place with tissue glue and exteriorized to the back. The abdomen was closed with 4-0 silk suture and tissue glue, and surgical tape was wrapped around the animal's trunk. After awakening from anesthesia, animals were allowed to walk on an exercise wheel; core temperature was maintained at 27-30°C with a heat lamp.

Mixed micelles were then infused at 5 μl/min through the duodenal cannula, and lymph samples were collected hourly. Aliquots of lymph (150 μl) were diluted to 2.0 ml with saline and centrifuged at 50,000 rpm for 4 h at 15°C in a Beckman TLA 120.2 rotor to float d < 1.006 g/ml chylomicrons. Chylomicrons were aspirated from the top of the tubes, rediluted to 500 μl, and assayed for TG concentration in duplicate using a colorimetric enzymatic assay (L-Type Triglyceride M, Wako Diagnostics, Richmond, VA).

Segmental lipid transport

Segmental intestinal lipid transport was examined using everted gut sacs (35), which measure transmucosal TG transport by the appearance of radioactivity in sac fluid. Animals maintained on chow were fasted for 12 h, anesthetized with ketamine and xylazine, and then euthanized. The entire small intestine from the pylorus to the cecum was excised and divided into four equal segments (hereafter identified as duodenum, jejunum I, jejunum II, and ileum). A 7 cm piece was cut from the middle of each segment, everted over a blunt 18 gauge needle, tied at one end with 4-0 silk suture, filled with 200 μl of DMEM buffer, carefully sealed with a second suture, and weighed. Sacs were then incubated at 37°C in 15 ml plastic tubes filled with 4.5 ml of an oxygenated solution of mixed micelles containing 0.1 μCi of [^{14}C]carboxy inulin. At timed intervals, sacs were removed, weighed, and opened, and the volume of fluid was measured. Empty sacs were flushed with DMEM, then weighed again and homogenized by incubation with 1 ml of 1M NaOH at 37°C for 2.5 h. Radioactivity in sac fluids and tissue homogenates was assayed by scintillation counting. [^{3}H]oleic acid uptake into tissue and secretion into sac fluid was calculated as nmol/g tissue. Sac viability and the presence of leaks were assessed by calculating bath/sac fluid [^{14}C] ratios, which were 9.6 ± 0.4 at 30 min, 7.6 ± 0.2 at 60 min, and 6.5 ± 0.4 at 90 min. Sacs in which the ratio was one standard deviation below the mean were rejected and excluded from analysis.

Characterization of secreted lipoproteins

Lipoproteins secreted into sac fluids at 60 min were isolated by centrifugation at 1.25 g/ml in a 51.3Ti rotor at 40,000 rpm for 12 h without braking. The floating top lipid layers (~150-200 μl) were collected and made 0.01% with sodium azide. Lipoproteins were analyzed with a Zetasizer® Nano-S Particle Analyzer at 633 nm (Malvern, Worcestershire, United Kingdom) to determine the intensity-weighted mean diameter and particle size distribution. Analysis of 1:0, 2:1, and 1:1 dilutions of sac fluids from the initial experiment revealed a minimal effect on the calculated particle size distribution; thus, samples were analyzed in triplicate without dilution thereafter. ApoB concentration at 60 min was measured by slot blotting, using a 1:1000 dilution of rabbit anti-mouse IgG apolipoprotein B (Meridian Life Science, Saco, ME) in PBS with 0.1% Tween and 2.5% nonfat dry milk as the primary antibody, and a 1:6000 dilution of horseradish peroxidase conjugated goat anti-rabbit IgG (Sigma-Aldrich) as the secondary antibody. ApoB band intensity was determined by chemiluminescence using SuperSignal® West Pico Chemiluminescent Substrate (Pierce, Rockford, IL) and a Fujifilm LAS 3000 Luminescent Image Analyzer. A series of dilutions of LDL receptor knockout mouse plasma containing a known concentration of apoB (545 μg/ml) served as standards. The apoB standard curve regression equation was y = 3290×, R = 0.982.

Intestinal gene expression

Intestines were harvested from separate groups of chow-fed animals after an overnight fast. Animals were anesthetized with ketamine and xylazine and then euthanized. The entire small intestine was excised and divided into four equal segments as described above. Segments were rinsed with PBS and snap frozen in liquid nitrogen. Frozen tissues were powdered using a metal mortar and pestle cooled by liquid nitrogen, and then sonicated in TRIzol (Invitrogen) using a Polytron PT 1200E (Kinematica, Bohemia, NY) at the highest power level for 30-60 s. Total RNA was extracted using TRIzol, chloroform, and isopropanol; quantitated by spectrophotometry; examined for integrity by 1% agarose gel electrophoresis; and converted into cDNA using Omniscript RT kits (Qiagen, Valencia, CA). RT-PCR was performed on a 7500 Fast Real Time PCR System (Applied Biosystems, Foster City, CA). A typical PCR reaction (20 μl) contained 10 μl 2× Fast SYBR Green Master Mix (Applied Biosystems), 1 μl each of 5 μM forward and reverse primers, and a 1:10 dilution of cDNA. Copy numbers were normalized to GAPDH or cyclophilin. The following primers were used: apoA-IV, forward TTC CTG AAG GCT GCG GTG CTG, reverse CTG CTG AGT GAC ATC CGT CTT CTG; apoB, forward CGT GGG CTC CAG CAT TCT A, reverse TCA CCA GTC ATT TCT GCC TTT G; microsomal triglyceride transfer protein (MTP), forward CCT ACC AGG CCC AAC AAG AC, reverse CGC TCA ATT TTG CAT GTA TCC; diacylglycerol acyltransferase-2 (DGAT2), forward CCG CAA AGG CTT TGT GAA G, reverse GGA ATA AGT GGG AAC CAG ATC A; intestinal fatty acid binding protein (FABP2), AGT CTA GCA GAC GGA ACG GA forward, AGA AAC CTC TCG GAC AGC AA reverse; CD36, CCA AGC TAT TGC GAC ATG ATT forward, TCT CAA TGT CCG AGA CTT TTC A reverse.

Weight gain, adiposity, and food consumption

To examine the effect of apoA-IV expression on weight gain, groups of male C57BL56 and A4KO mice, 3 to 4 months old, were fed either rodent chow (ProLab RMH 3000, PMI Nutrition), which provided 26% of calories from protein, 60% from carbohydrate, 14% from fat, and 3.2 Kcal/g, or a high-fat diet (TD88137, Harlan Teklad, Indianapolis, IN), which provided 15.2% of calories from protein (casein), 42.7% of calories from carbohydrate (sucrose and corn starch), 42% of calories from anhydrous milk fat, and 4.5 Kcal/g, for 12 weeks. A single lot of each was used throughout the study to minimize lot-to-lot variability. Animals were given ad libitum access to both food and water, and they were weighed weekly. At the end of the feeding period, animals were anesthetized with ketamine and xylazine and euthanized. Epididymal fat pads, livers, and intestines were removed and weighed. To assess daily food consumption, separate groups (n = 4) of male C57BL56 and A4KO mice, 3 to 4 months old, were housed in individual cages with wire mesh floors and provided weighed amounts of food in small cups nightly for one week. Uneaten food in the cups and food collected from the cage bottoms were combined and weighed each morning. Daily food consumption for each animal was calculated as the difference between the weight of the nightly ration and total uneaten food.

Plasma gut hormone levels

Separate groups (n = 3) of C57BL6 and A4KO mice were fed chow or a high-fat diet for one week. Postprandial plasma obtained in the morning was assayed for glucagon-like peptide-1 (GLP-1) and PYY levels using enzyme immunoassay kits and standards from Phoenix Pharmaceuticals (Burlingame, CA).

Statistical analysis

Statistical analysis was performed using Sigma Stat 3.00 (Systat Software, San Jose, CA). Data are expressed as mean ± SEM. Differences in values among groups were analyzed by

one-way ANOVA (ANOVA) with Holm-Sidak multiple comparison post hoc testing. Differences were considered significant at $P < 0.05$.

RESULTS

Dietary fatty acid absorption

Reasoning that the effect of apoA-IV on intestinal fat absorption might become evident under conditions of a high dietary fat intake, we measured the efficiency of dietary FA absorption in C57BL6 and A4KO mice using the Olestra® method (32). As previously observed (36), various dietary fatty acids were absorbed with different efficiencies in both strains (**Fig. 1**). Myristic (14:0), linoleic (18:3), eicosapentaenoic (20:5), and docosahexaenoic (22:6) acids were absorbed with near 100% efficiency, but other fatty acids were absorbed less efficiently in the following order: stearic acid (C18:0) < linoleic acid (18:2) < palmitic (16:0) and oleic acids (18:1). However, there was no significant difference in the absorption efficiency of any fatty acid between the C57BL6 and A4KO mice with the exception of oleic acid, for which the absorption efficiency was slightly higher in the A4KO mice. Total dietary TG absorption, calculated by summing all fatty acids for each animal, was 98.3% ± 0.04% for C57BL6 mice and 98.3% ± 0.12% for A4KO mice. These data establish that apoA-IV gene expression has a negligible impact on the intestinal absorption of dietary fatty acids and total fat in mice fed a synthetic high-fat diet.

Lymph duct cannulation

With infusion of mixed micelles in saline into the duodenum, lymph flows of 206 ± 25 μl/hr and 183 ± 15 μl/hr were obtained in C57BL6 and A4KO mice, respectively. There was no significant difference between the strains in cumulative chylomicron TG output into lymph (**Fig. 2**). As the lymphatic system integrates lipid absorption from the entire gut, these data corroborate the dietary fatty acid absorption study and suggest that total intestinal fat absorption is not impaired in A4KO mice.

Segmental lipid absorption

Regional intestinal lipid absorption and transport were measured using everted gut sacs. There was no significant difference between C57BL6 and A4KO mice in tissue [^{3}H] oleate uptake over time, with the exception of a transiently higher uptake in the jejunum I segment in the A4KO mice at 30 min (**Fig. 3**). In both C57BL6 and A4KO mice, oleate secretion into sac fluid increased over time in all segments, and was highest in jejunum I and lowest in the ileum at all times (**Fig. 4**). At 30 and 60 min, there were no significant differences between the two strains in regional lipid secretion. However, at 90 min, lipid transport had become significantly higher in the jejunum I segment in the C57BL6 mice. These data establish that although apoA-IV gene expression did not affect uptake of fatty acids from the lumen into intestinal mucosa, it facilitated TG secretion from the mucosa into the basolateral medium in the proximal jejunal sacs.

Characterization of secreted lipoproteins

As TG-rich lipoproteins contain only one apoB molecule per particle (37), apoB concentration in gut sac fluids was determined to provide a surrogate measure of the number of secreted lipoprotein particles. In both C57BL6 and A4KO mice, apoB concentration was highest in sac fluid from jejunum I and lowest in the ileum; however, apoB concentration was significantly higher in both jejunum I and II in the C57BL6 mice (**Table 1**), indicating that apoA-IV expression increased the number of particles secreted by jejunal gut sacs. Laser light scattering analysis of lipoproteins secreted into sac fluids revealed that the intensity-weighted mean particle diameter in both C57BL6 and A4KO mice was largest in the duodenum (Table 1). In C57BL6 mice, mean particle diameters were smaller, but similar, in jejunum I, jejunum II, and ileal segments. However, in A4KO mice, lipoproteins secreted in the jejunum II and ileum segments were smaller than lipoproteins secreted in the proximal segments, such that they were significantly different from C57BL6. Because intensity-weighted mean diameter is calculated from light scattering intensity, which is a function of the sixth power of

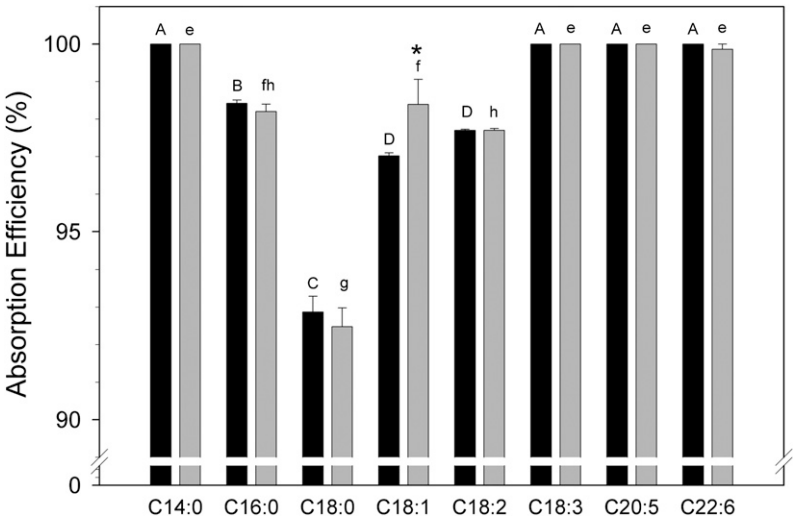

Fig. 1. Efficiency of intestinal fatty acid absorption in C57BL6 (black bars) and A4KO (gray bars) mice determined using sucrose polybehenate as a nonabsorbable marker. Bar heights are means ± SEM, n = 5 in each group. Bars for each strain marked with different superscripts (C57BL6, capital letters A–D; A4KO, lowercase letters e–h) are different at $P = 0.001$ by ANOVA. Pairs of absorption values for individual fatty acids marked with an asterisk are significantly different between the two stains.

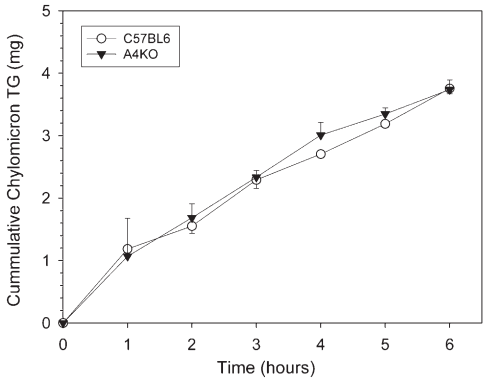

Fig. 2. Cumulative chylomicron TG output into mesenteric lymph in C57BL6 (○) and A4KO (▼) mice during a constant duodenal infusion of [^{3}H]oleate labeled mixed micelles. Data points are means ± SEM, n = 4 in each group.

particle diameter, it is disproportionately affected by the presence of larger particles. Therefore, we examined the lipoprotein particle size distribution in sac fluids (**Fig. 5**). Three broad particle size ranges were noted (38): small VLDL particles with a peak centered at 25 nm; larger VLDL particles with a peak centered at 44 nm; and chylomicron-sized particles with a peak centered at 295 nm. ApoA-IV expression altered the particle size distribution in a regionally specific manner. In the duodenum, chylomicron-sized particles constituted the greatest volume percentage in both C57BL6 and A4KO mice, although A4KO mice secreted a smaller percentage in the large VLDL range. In jejunum I, both C57BL6 and A4KO mice displayed mixed populations of chylomicrons and large VLDL, although the peak widths were much broader in the C57BL6 mice. Both strains similarly displayed the largest percentage of small VLDL in jejunum II and large VLDL in ileum; however, sac fluids from C57BL6 jejunum II and ileum contained a higher percentage of the larger chylomicrons. These data indicate that in the proximal gut, apoA-IV expression increases the number of secreted TG-rich lipoproteins particles, but in the distal gut, apoA-IV expression is associated with secretion of a discrete population of larger chylomicrons.

Intestinal gene expression

ApoA-IV gene expression in C57BL6 mice was highest in the duodenum and decreased in a proximal-to-distal gradient along the small bowel; ileal expression was less than 7% of that in the duodenum (**Fig. 6A**); as expected, apoA-IV gene expression was undetectable in the A4KO mice. In C57BL6 mice, apoB gene expression was constant among all intestinal segments, whereas MTP was highest in jejunum I, DGAT2 and CD36 were highest in the proximal gut segments, and FABP2 was highest in jejunum II. In A4KO mice, apoB, MTP, DGAT, FABP2, and CD36 gene expression was elevated 3.5-fold in each segment; was highest in jejunum I; and declined progressively toward the distal gut (Fig. 6B, C, E, F), except for FABP2, which was highest in jejunum II. (Fig. 6D). These data

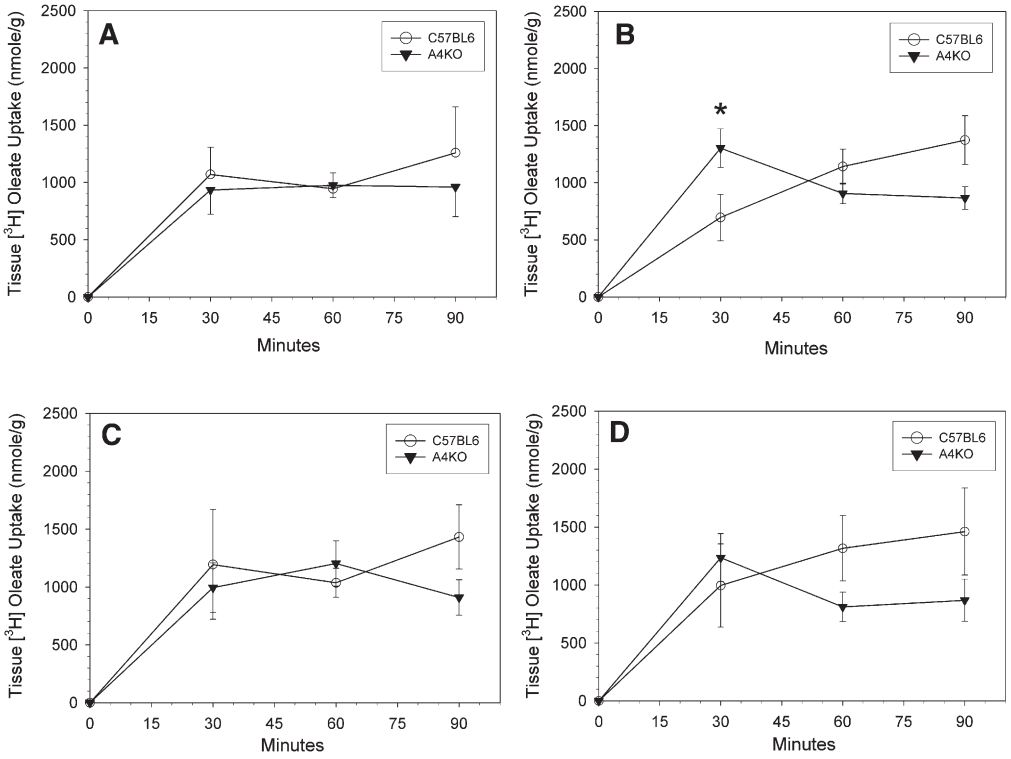

Fig. 3. Time course of regional [^{3}H]oleate uptake into gut sac tissue in C57BL6 (○) and A4KO (▼) mice. Data points are means ± SEM, n = 3-10. Data points at each time marked with an asterisk are significantly different at $P < 0.001$ between the two stains by ANOVA. Panel A, duodenum; panel B, jejunum I; panel C, jejunum II; panel D, ileum.

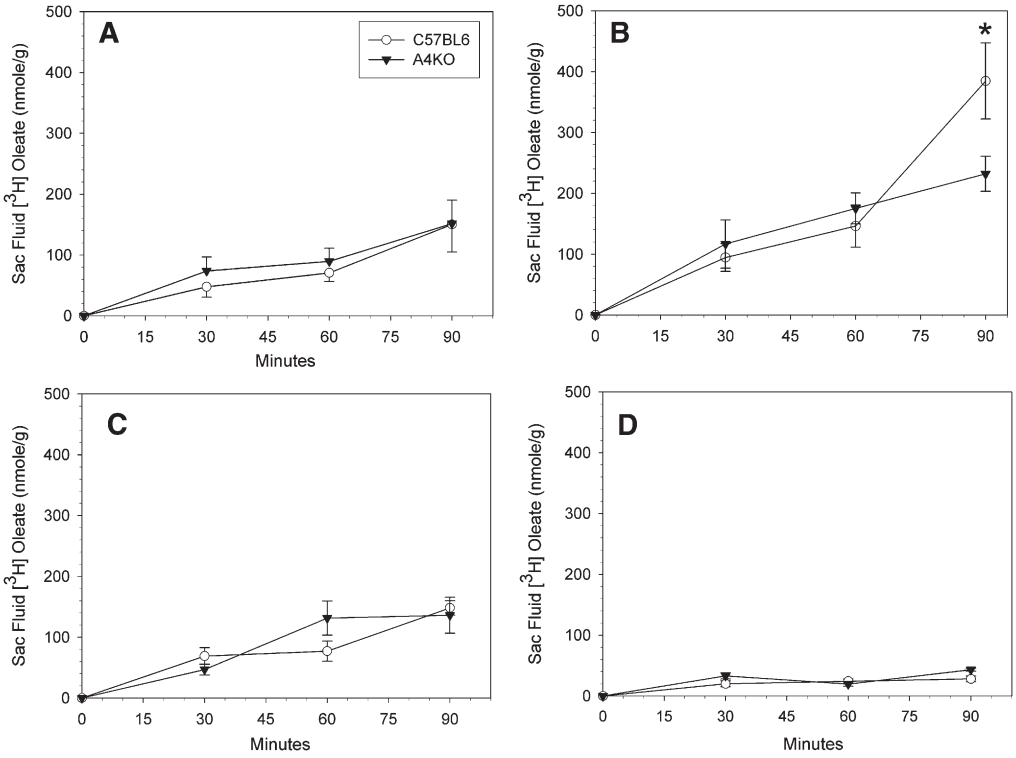

Fig. 4. Regional secretion of [^{3}H]oleate into gut sac fluids in C57BL6 (○) and A4KO (▼) mice. Data points are means ± SEM, n = 3-10. Data points at each time marked with an asterisk are significantly different at $P = 0.001$ between the two stains by ANOVA. Panel A, duodenum; panel B, jejunum I; panel C, jejunum II; panel D. ileum.

establish that inactivation of apoA-IV expression is associated with upregulation of the genes for key proteins involved in chylomicron assembly.

Weight gain, adiposity, and food consumption

Over the course of 12 weeks on a chow diet, C57BL6 mice gained less weight than A4KO mice (**Fig. 7**), such that mean daily weight gain over the 12-week study was lower, 130.2 ± 0.9 mg/day versus 147.5 ± 0.9 mg/day (**Table 2**). However, on the high-fat diet, C57BL6 mice gained significantly more weight than A4KO mice, beginning at week 5, such that the difference in mean daily weight gain, 219.3 ± 2.5 versus 145.6 ± 1.5, was highly significant ($P < 0.001$). Thus, whereas C57BL6 mice gained significantly more weight on the high-fat diet compared with chow, weight gain in the apoA-IV knockout mice was the same on both diets. After 12 weeks on chow, there was no significant difference in epididymal fat pad weight between the C57BL6 and A4KO mice; however, after 12 weeks on the high-fat diet, the fat pad weight was almost 2-fold greater in the C57BL6 mice (**Fig. 8**). There was no difference in liver or intestinal weight between the C57BL6 and A4KO mice on either diet, although intestinal weights were lower in both strains on the high-fat diet.

As apoA-IV has been proposed to function as a satiety factor (23), we measured food consumption on both diets in separate cohorts of animals. We observed no significant difference in daily food consumption among the four treatment groups (Table 2, $P = 0.434$). These data are in accord with findings in earlier studies that neither overexpression of a human apoA-IV transgene (28) nor deletion of the murine apoA-IV gene (29) significantly altered food

TABLE 1. Gut sac fluid apoB concentration and intensity-weighted mean lipoprotein diameter

	Duodenum	Jejunum I	Jejunum II	Ileum
Apolipoprotein B *μg/ml/μg tissue*				
C57BL6	120.4 ± 60.7^{AC}	$278.4 \pm 36.7^{B\#}$	$164.0 \pm 76.9^{A\#}$	4.8 ± 1.4^{C}
A4KO	43.9 ± 7.5^{A}	121.9 ± 12.9^{B}	45.5 ± 33.9^{AB}	6.6 ± 2.8^{A}
Particle diameter *nm*				
C57BL6	185.9 ± 5.1^{A}	154.0 ± 4.5^{B}	$150.7 \pm 7.1^{B\#}$	$142.7 \pm 7.2^{B\#}$
A4KO	188.8 ± 3.8^{A}	166.4 ± 5.9^{B}	126.4 ± 5.8^{C}	114.7 ± 2.0^{C}

Measurements were performed on sac fluids obtained at 60 min. Means ± SEM, n = 3 for each group. Values in each row with different superscripts are different at $P = 0.002$ for sac fluid apoB concentration and $P < 0.001$ for the intensity-weighted mean diameter of secreted lipoproteins by ANOVA. Pairs of values in each column marked by # are significantly different between the two stains.

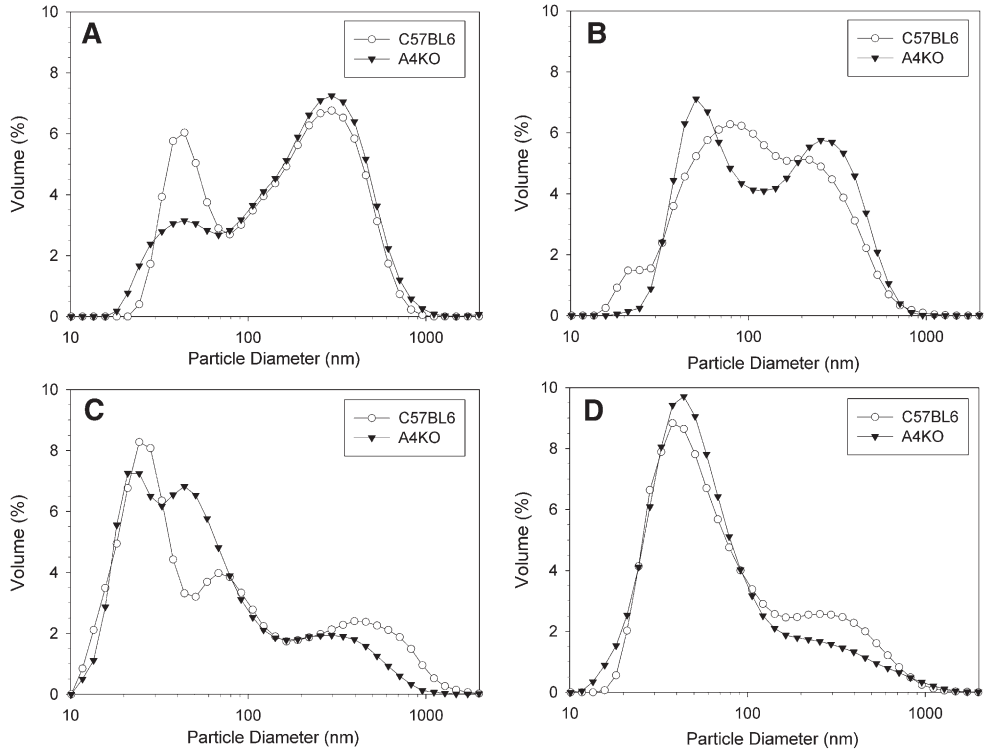

Fig. 5. Size distributions of d < 1.21 g/ml lipoproteins secreted into gut sacs in C57BL6 (○) and A4KO (▼) mice determined by dynamic laser light scattering. Data points are means, n = 3. Panel A, duodenum; panel B, jejunum I; panel C, jejunum II; panel D, ileum.

intake. Extrapolating the food consumption data to the weight gain study enabled calculation of weight gained per kilocalorie of food consumed, a measure of the efficiency of food energy utilization and storage. This calculation revealed that although there was no difference in food energy storage efficiency between the two strains on the chow diet, the A4KO mice were less efficient in storing food energy when fed a high-fat diet (Table 2). These data suggest that apoA-IV gene expression promotes positive energy balance in the setting of a high-fat intake.

Plasma gut hormone levels

The secretion of the gut hormones GLP-1 and PYY is stimulated by the presence of fatty acids in the lumen of the distal gut (39–41). On a chow diet, plasma GLP-1 and PYY levels were similar in C57BL6 and A4KO mice (**Fig. 9**). However, after one week on a high-fat diet, plasma GLP-1 and PYY levels were significantly higher in the A4KO mice. These data provide evidence for an effect of apoA-IV expression on the efficiency of proximal lipid absorption in vivo.

DISCUSSION

Studies over the past three decades have consistently supported a central role of apoA-IV in intestinal lipid absorption (13–22). Nonetheless, the conundrum has remained that the seminal study in A4KO mice found no impairment in intestinal lipid absorption (29). In an attempt to reconcile these conflicting observations, we first considered that the use of postprandial plasma TG appearance curves and retinol ester ratios as measures of intestinal fat absorption efficiency in this study did not have sufficient sensitivity to detect subtle effects of the apoA-IV gene deletion. However, using the sensitive sucrose polybehenate fat balance method (32), we confirmed that A4KO mice absorb dietary fatty acids with the same efficiency as C57BL6 control mice, even when challenged with a diet containing a high-fat content. Similarly, lymph duct cannulation studies observed no difference between C57BL6 and A4KO mice in the appearance of infused fatty acids as mesenteric lymph chylomicron TG. Together these data strongly suggest that the effects of apoA-IV expression on intestinal lipid absorption cannot be detected by techniques that measure the integrated absorptive function of the entire small bowel.

The small bowel displays functional heterogeneity along its length. Different dietary constituents are absorbed with highest efficiency in different anatomic regions; for example, iron is preferentially absorbed in the duodenum, vitamin B12 is absorbed exclusively in the ileum, and lipids are primarily absorbed in the proximal half of the gut with very high efficiency (>95%) (42). Thus, we next considered the possibility that the ability of apoA-IV to facilitate TG absorption at the cellular level might be manifest in the intestine only at the suborgan level. By measuring TG transport in everted gut sacs from different regions of the small bowel, we found that apoA-IV expression increases bulk TG transport only in the proximal jejunum. As apoA-IV expression had little impact on mucosal fatty acid

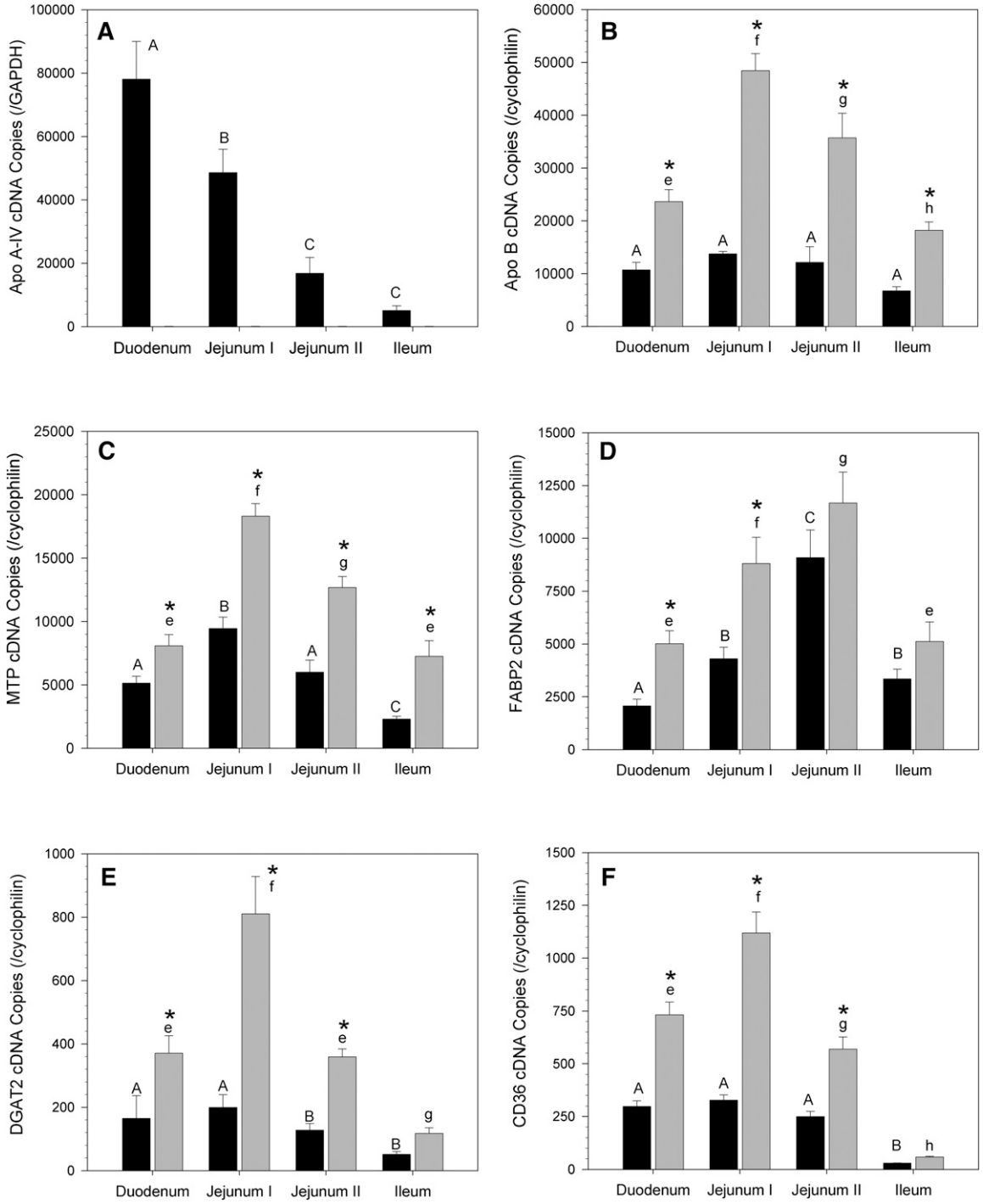

Fig. 6. RT-PCR copy numbers in gut sac mucosa for apoA-IV and key genes involved in triglyceride absorption for C57BL6 (black bars) and A4KO (gray bars) mice. Copy numbers are normalized to GAPDH (apoA-IV) or cyclophilin (all other genes). Bar heights are means ± SEM, n = 3 for each group. Bars for each strain marked with different superscripts (C57BL6, capital letters A–D; A4KO, lowercase letters e–h) are different at $P = 0.001$ by ANOVA. Pairs of absorption values at each anatomic region marked with an asterisk are significantly different between the two stains. Panel A, apoA-IV; panel B, apoB; panel C, MTP; panel D, FABP2; panel E, DGAT2; panel F, CD36.

uptake, its ability to increase TG transport in the proximal gut must be due to an effect on lipid export. The action of apoA-IV on TG transport and apoB secretion, a biological marker of the number of secreted apoB-containing lipoproteins, was greatest in the proximal jejunum, where MTP gene expression was highest, not in the duodenum, where apoA-IV gene expression was highest. As MTP plays an essential role in the first step of apoB lipidation during the assembly of TG-rich lipoproteins (37, 43), this suggests that apoA-IV may have increased the efficiency of initial apoB lipidation. In this regard, in studies in COS cells cotransfected with a KDEL-modified apoA-IV, MTP, and a series of apoB constructs, we showed that apoA-IV interacts with some of the smallest apoB truncations capable of

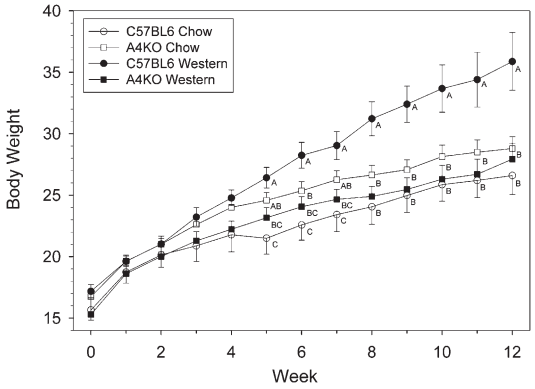

Fig. 7. Weight gain in C57BL6 (○) and A4KO (□) mice fed chow and C57BL6 (●) and A4KO (■) mice fed a high-fat diet for 12 weeks. Data points are means ± SEM, n = 4-11 per group. Weights at each time point marked with different letters are significantly different at $P < 0.01$ by ANOVA.

TG-rich lipoprotein assembly (44), suggesting that it might facilitate apoB lipidation by acting as a molecular chaperone in the early stage of apoB endoplasmic reticulum (ER) translocation. Moreover, we have observed in McRH-7777 rat hepatoma cells that apoA-IV delays apoB secretion kinetics (44), suggesting that it could increase the efficiency of apoB lipidation by prolonging the residence of nascent lipoproteins in cellular compartments where lipidation occurs.

Given the importance of interfacial phenomena in the initiation of TG-rich particle assembly (45, 46) and the finding that apoA-IV displays the highest dynamic interfacial elasticity of any apolipoprotein (20), we have proposed that apoA-IV might increase the efficiency of intestinal lipid absorption by facilitating particle expansion during the second step of TG-rich lipoprotein assembly (20). The observation that apoA-IV expression in IPEC-1 intestinal cells increases the size of secreted TG-rich lipoproteins supports this hypothesis (22). However, in the present study, the effect of apoA-IV on lipoprotein size was subtle and confined to the distal jejunum and ileum. This disparity could be caused by differences between the expression of genes involved in enterocyte lipid transport in cell culture and their regional expression in vivo, or it could be because apoA-IV expression in the IPEC-1 cell studies was under control of a TET-inducible promoter and not under physiological regulation. In any case, if the effect of apoA-IV on lipid transport observed in gut sacs is maintained in vivo (i.e., apoA-IV expression facilitates secretion of a greater number of lipoprotein particles in the proximal gut), the ultimate consequence would be to maintain a proximal-to-distal gradient of lipid absorption efficiency that prevents the majority of dietary lipids from reaching the distal gut. The metabolic implications of this will be discussed below.

TABLE 2. Weight gain, food intake, and food energy storage

	Weight gain	Food intake	Energy intake	Energy storage
	mg/day	*g/day*	*Kcal/day*	*mg/Kcal*
Chow diet				
C57BL6	130.2 ± 0.9^{A}	3.54 ± 0.20	11.3 ± 0.6^{A}	11.6 ± 1.2^{AB}
A4KO	147.5 ± 0.9^{B}	3.66 ± 0.16	11.7 ± 0.5^{A}	12.5 ± 1.0^{A}
High-fat diet				
C57BL6	219.3 ± 2.5^{C}	3.91 ± 0.27	17.6 ± 1.2^{B}	12.5 ± 1.9^{A}
A4KO	145.6 ± 1.5^{B}	4.01 ± 0.23	18.0 ± 1.0^{B}	8.1 ± 1.1^{B}

Means ± SEM, n = 4-11 animals per group. Values in each column with different superscripts are $P < 0.001$ for weight gain and energy intake; $P = 0.039$ for energy storage by ANOVA.

In a recent review of the molecular mechanisms intestinal lipid absorption, Black speculated that a possible explanation for the absence of a malabsorption phenotype in A4KO mice was compensatory upregulation of other key genes involved in chylomicron assembly and secretion (47). Assessment of apoB, MTP, DGAT2, FABP2, and CD36 mRNA levels along the intestine by RT-PCR revealed that expression of all of these was increased in A4KO mice, albeit with regional differences in fold elevation. As these genes all reside on different chromosomes from apoA-IV (apoA-IV, chromosome 9; apoB, chromosome 12; MTP, chromosome 3; DGAT2, chromosome 7; FABP2, chromosome 3; CD36, chromosome 5), these changes are unlikely to be an artifact of the construction of the A4KO mouse (29). On the other hand, as the promoters for some of these genes contain regulatory elements for hepatocyte nuclear factor 4 alpha (HNF4α) and peroxisome proliferator-activated receptors (PPAR) (43, 48, 49), which can bind fatty acids, the altered secretion kinetics of absorbed fatty acids, especially in the proximal gut, may have increased transcription of these genes. To the extent that apoA-IV plays a critical role in lipid absorption, the upregulation of these genes in the A4KO mouse intestine may have compensated for the absence of apoA-IV and prevented the appearance of gross fat malabsorption. Studies in apoA-IV double-knockout mice bearing mutations that impair the activity of genes involved in chylomicron assembly will be necessary to confirm this conjecture.

Recent data from animal and human studies have established that the site of nutrient absorption along longitudinal gut axis can have a profound impact on energy utilization and storage (39). Thus, the ability of apoA-IV to modulate regional TG absorption could have major metabolic consequences. We observed that over the course of 12 weeks on a high-fat diet, but not on a chow diet with a lower fat content, A4KO mice gained less weight and had lower final adiposity than C57BL6 mice, despite consuming and absorbing the same amount of dietary fat. Moreover, the calculated daily weight gained per kilocalorie consumed on the high-fat diet was significantly lower for A4KO mice than for C57BL6 mice. With the caveat that we did not measure activity levels in these animals, these data suggest that intestinal apoA-IV expression can modulate energy balance. How could this be? The distal gut contains populations of L-cells, which are specialized neuroendocrine cells that in the presence of luminal fatty acids secrete PYY and GLP-1, which are potent gastrointestinal hormones that suppress appetite (39) and increase basal metabolic rate (40, 41). In C57BL6 mice fed a high-fat diet, meal-stimulated apoA-IV synthesis would both increase

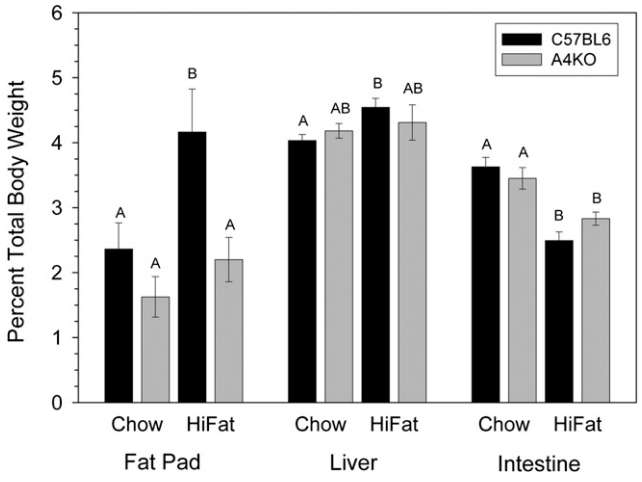

Fig. 8. Epididymal fat pad and organ weights in C57BL6 (black bars) and A4KO (gray bars) mice after 12 weeks on a chow or a high-fat diet. Bar heights are means ± SEM, n = 4-9 per group. Bars for each tissue with different superscripts are different at $P = 0.002$ by ANOVA.

proximal TG transport and delay gastric emptying (50), thus limiting the amount of dietary fatty acids reaching the distal gut. However, in the A4KO mice, impaired proximal TG transport and increased gastric emptying (51) could enable dietary fatty acids to reach the ileum and stimulate secretion of PYY and GLP-1, as suggested by the increased levels of these hormones in A4KO mice fed a high-fat diet. Not only would increased secretion of PYY and GLP-1 increase basal energy expenditure and impede weight gain but their central anorexic action could explain why A4KO mice do not exhibit hyperphagia compared with C57BL6 mice, as might be expected if apoA-IV functioned as a classical meal-responsive satiety factor.

In conclusion, although fat balance, lymph duct cannulation, and food intake studies confirmed that deletion of the apoA-IV gene has no impact on total dietary fat absorption or food intake, studies with intestinal gut sacs revealed that intestinal apoA-IV gene expression facilitates TG transport in the proximal gut by increasing the number of secreted TG-rich lipoproteins. Feeding studies revealed that, in the setting of a high dietary fat intake, apoA-IV facilitates weight gain and adipose tissue lipid storage, possibly by limiting the entry of dietary fatty acids into the distal gut, thereby attenuating secretion of gut hormones that suppress appetite and increase basal energy expenditure. Considering our observations in the light of past research on apoA-IV, we propose that by functioning as a nutrient-responsive modulator (15) of regional TG absorption and foregut motility (50, 51), apoA-IV stands at the nexus of a complex neuroendocrine system that integrates feeding behavior, intestinal function, and energy utilization and storage. The function of apoA-IV in this system could help maintain positive energy balance during times of high lipid loads (e.g., in neonates) or impaired intestinal function (e.g., poststarvation [52]). Future studies will explore the unique metabolic effects of this fascinating apolipoprotein.

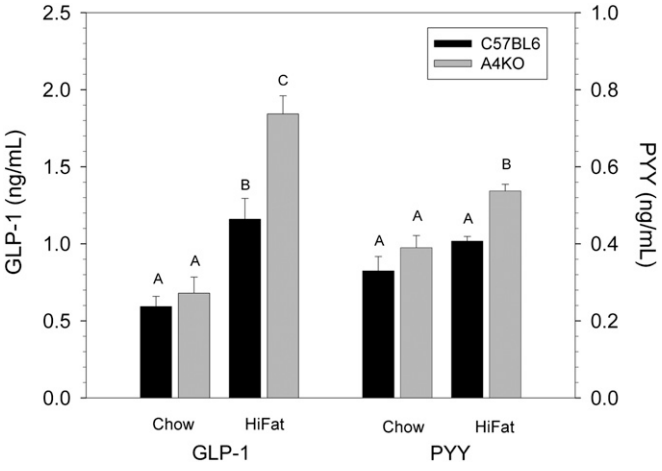

Fig. 9. Plasma GLP-1 and PYY levels in C57BL6 (black bars) and A4KO (gray bars) mice after one week on a chow or a high-fat diet. Bar heights are means ± SEM, n = 3 per group. Bars for each hormone with different superscripts are different at $P < 0.001$ for GLP-1 and $P = 0.002$ for PYY by ANOVA.

The authors thank Tam Nguyen and Janet K. Sawyer for technical assistance with the lymph duct cannulation surgery.

REFERENCES

1. Luo, C. C., W. H. Li, M. N. Moore, and L. Chan. 1986. Structure and evolution of the apolipoprotein multigene family. *J. Mol. Biol.* **187:** 325–340.
2. Green, P. H., R. M. Glickman, J. W. Riley, and E. Quinet. 1980. Human apolipoprotein A-IV: intestinal origin and distribution in plasma. *J. Clin. Invest.* **65:** 911–919.
3. Hayashi, H., D. F. Nutting, K. Fujimoto, J. A. Cardelli, D. D. Black, and P. Tso. 1990. Transport of lipid and apolipoproteins apo A-I and apo A-IV in intestinal lymph of the rat. *J. Lipid Res.* **31:** 1613–1625.
4. Swaney, J. B., H. Reese, and H. A. Eder. 1974. Polypeptide composition of rat high density lipoprotein: characterization by SDS-gel electrophoresis. *Biochem. Biophys. Res. Commun.* **59:** 513–519.
5. Lefevre M., and P. S. Roheim. Metabolism of apolipoprotein A-IV. 1984. *J. Lipid Res.* **25:** 1603–1610.
6. Stan, S., E. Delvin, M. Lambert, E. Seidman, and E. Levy. 2003. Apo A-IV: an update on regulation and physiologic functions. *Biochim. Biophys. Acta.* **1631:** 177–187.
7. Steinmetz, A., and G. Utermann. 1985. Activation of lecithin-cholesterol acyltransferase by human apolipoprotein A-IV. *J. Biol. Chem.* **260:** 2258–2264.
8. Goldberg, I. J., C. A. Scheraldi, L. K. Yacoub, U. Saxena, and C. L. Bisgaier. 1990. Lipoprotein apoC-II activation of lipoprotein lipase. Modulation by apolipoprotein A-IV. *J. Biol. Chem.* **265:** 4266–4272.
9. Weinberg, R. B., R. A. Anderson, V. R. Cook, F. Emmanuel, P. Denefle, A. R. Tall, and A. Steinmetz. 2002. Interfacial exclusion pressure determines the ability of apolipoprotein A-IV truncation mutants to activate cholesterol ester transfer protein. *J. Biol. Chem.* **277:** 21549–21553.
10. Bielicki, J. K., W. J. Johnson, R. B. Weinberg, J. M. Glick, and G. H. Rothblat. 1992. Efflux of lipid from fibroblasts to apolipoproteins: dependence on elevated levels of cellular unesterifed cholesterol. *J. Lipid Res.* **33:** 1699–1709.
11. Qin, X., D. K. Swertfeger, S. Zheng, D. Y. Hui, and P. Tso. 1998. Apolipoprotein AIV: a potent endogenous inhibitor of lipid oxidation. *Am. J. Physiol.* **274:** H1836–H1840.
12. Recalde, D., M. A. Ostos, E. Badell, A. L. Garcia-Otin, J. Pidoux, G. Castro, M. M. Zakin, and D. Scott-Algara. 2004. Human apolipoprotein A-IV reduces secretion of proinflammatory cytokines and atherosclerotic effects of a chronic infection mimicked by lipopolysaccharide. *Arterioscler. Thromb. Vasc. Biol.* **24:** 756–761.

13. Kumar, S., and S. B. Hedges. 1998. A molecular timescale for vertebrate evolution. *Nature.* **392:** 917–920.
14. Van der Horst, D. J., S. D. Roosendaal, and K. W. Rodenburg. 2009. Circulatory lipid transport: lipoprotein assembly and function from an evolutionary perspective. *Mol. Cell. Biochem.* **326:** 105–119.
15. Kalogeris, T. J., M. D. Rodriquez, and P. Tso. 1997. Control of synthesis and secretion of intestinal apolipoprotein A-IV. *J. Nutr.* **127:** 537S–543S.
16. Kalogeris, T. J., K. Fukagawa, and P. Tso. 1994. Synthesis and lymphatic transport of intestinal apo A-IV in response to graded doses of triglyceride. *J. Lipid Res.* **35:** 1141–1151.
17. Kalogeris, T. J., F. Monroe, S. J. Demichele, and P. Tso. 1996. Intestinal synthesis and lymphatic secretion of apolipoprotein A-IV vary with chain length of intestinally infused fatty acids in rats. *J. Nutr.* **126:** 2720–2729.
18. Tso, P., J. A. Balint, M. B. Bishop, and J. B. Rodgers. 1981. Acute inhibition of intestinal lipid transport by Pluronic L-81 in the rat. *Am. J. Physiol.* **241:** G487–G497.
19. Kumar, N. S., and C. M. Mansbach 2nd. 1999. Prechylomicron transport vesicle: isolation and partial characterization. *Am. J. Physiol.* **276:** G378–G386.
20. Weinberg, R. B., V. R. Cook, J. A. DeLozier, and G. S. Shelness. 2000. Dynamic interfacial properties of human apolipoproteins A-IV and B17 at the air/water and oil/water interface. *J. Lipid Res.* **41:** 1419–1427.
21. Koga, S., Y. Miyata, A. Funakoshi, and H. Ibayashi. 1985. Plasma apolipoprotein A-IV levels decrease in patients with chronic pancreatitis and malabsorption syndrome. *Digestion.* **32:** 19–24.
22. Lu, S., Y. Yao, X. Cheng, S. Mitchell, S. Leng, S. Meng, J. W. Gallagher, G. S. Shelness, G. S. Morris, J. Mahan, et al. 2006. Over-expression of apolipoprotein A-IV enhances lipid secretion in IPEC-1 cells by increasing chylomicron size. *J. Biol. Chem.* **281:** 3473–3483.
23. Tso, P., W. Sun, and M. Liu. 2004. Gastrointestinal satiety signals IV. Apolipoprotein A-IV. *Am. J. Physiol. Gastrointest. Liver Physiol.* **286:** G885–G890.
24. Whited, K. L., P. Tso, and H. E. Raybould. 2007. Involvement of apolipoprotein A-IV and cholecystokinin1 receptors in exogenous peptide YY3–36-induced stimulation of intestinal feedback. *Endocrinology.* **148:** 4695–4703.
25. Fujimoto, K., K. Fukagawa, T. Sakata, and P. Tso. 1993. Suppression of food intake by apolipoprotein A-IV is mediated through the central nervous system in rats. *J. Clin. Invest.* **91:** 1830–1833.
26. Doi, T., M. Liu, R. J. Seeley, S. C. Woods, and P. Tso. 2001. Effect of leptin on intestinal apolipoprotein AIV in response to lipid feeding. *Am. J. Physiol. Regul. Integr. Comp. Physiol.* **281:** R753–R759.
27. Kalogeris, T. J., X. Qin, W. Y. Chey, and P. Tso. 1998. PYY stimulates synthesis and secretion of intestinal apolipoprotein AIV without affecting mRNA expression. *Am. J. Physiol.* **275:** G668–G674.
28. Aalto-Setälä, K., C. L. Bisgaier, A. Ho, K. A. Kieft, M. G. Traber, H. J. Kayden, R. Ranakrishnan, A. Walsh, A. D. Essenburg, and J. L. Brewlow. 1994. Intestinal expression of human apolipoprotein A-IV in transgenic mice fails to influence dietary lipid absorption or feeding behavior. *J. Clin. Invest.* **93:** 1776–1786.
29. Weinstock, P. H., C. L. Bisgaier, T. Hayek, K. Aalto-Setala, E. Sehayek, L. Wu, P. Sheiffele, M. Merkel, A. D. Essenburg, and J. L. Breslow. 1997. Decreased HDL cholesterol levels but normal lipid absorption, growth, and feeding behavior in apolipoprotein A-IV knockout mice. *J. Lipid Res.* **38:** 1782–1794.
30. Xie, Y., F. Nassir, J. Luo, K. Buhman, and N. O. Davidson. 2003. Intestinal lipoprotein assembly in apobec-1$^{-/-}$ mice reveals subtle alterations in triglyceride secretion coupled with a shift to larger lipoproteins. *Am. J. Physiol. Gastrointest. Liver Physiol.* **285:** G735–G746.
31. Mansbach 2nd, C. M., R. S. Cohen, and P. B. Leff. 1975. Isolation and properties of the mixed lipid micelles present in intestinal content during fat digestion in man. *J. Clin. Invest.* **56:** 781–791.
32. Jandacek, R. J., J. E. Heubi, and P. Tso. 2004. A novel, noninvasive method for the measurement of intestinal fat absorption. *Gastroenterology.* **127:** 139–144.
33. Brown, J. M., S. Chung, J. K. Sawyer, C. Degirolamo, H. M. Alger, T. Nguyen, X. Zhu, M. N. Duong, A. L. Wibley, R. Shah, et al. 2008. Inhibition of stearoyl-coenzyme A desaturase 1 dissociates insulin resistance and obesity from atherosclerosis. *Circulation.* **118:** 1467–1475.
34. Ionac, M., T. Laskay, D. Labahn, G. Geisslinger, and W. Solbach. 1997. Improved technique for cannulation of the murine thoracic duct: a valuable tool for the dissection of immune responses. *J. Immunol. Methods.* **202:** 35–40.
35. Wilson, T. H., and G. Wiseman. 1954. The use of sacs of everted small intestine for the study of the transference of substances from the mucosal to the serosal surface. *J. Physiol.* **123:** 116–125.
36. Labonté, E. D., L. M. Camarota, J. C. Rojas, R. J. Jandacek, D. E. Gilham, J. P. Davies, Y. A. Ioannou, P. Tso, D. Y. Hui, and P. N. Howles. 2008. Reduced absorption of saturated fatty acids and resistance to diet-induced obesity and diabetes by ezetimibe-treated and Npc1l1$^{-/-}$ mice. *Am. J. Physiol. Gastrointest. Liver Physiol.* **295:** G776–G783.
37. Shelness, G. S., and A. S. Ledford. 2005. Evolution and mechanism of apolipoprotein B-containing lipoprotein assembly. *Curr. Opin. Lipidol.* **16:** 325–332.
38. Colhoun, H. M., J. D. Otvos, M. B. Rubens, M. R. Taskinen, S. R. Underwood, and J. H. Fuller. 2002. Lipoprotein subclasses and particle sizes and their relationship with coronary artery calcification in men and women with and without type 1 diabetes. *Diabetes.* **51:** 1949–1956.
39. Woods, S. C. 2006. Dietary synergies in appetite control: distal gastrointestinal tract. *Obesity (Silver Spring).* **14(Suppl 4):** 171S–178S.
40. Kirchner, H., J. Tong, M. H. Tschöp, and P. T. Pfluger. 2010. Ghrelin and PYY in the regulation of energy balance and metabolism: lessons from mouse mutants. *Am. J. Physiol. Endocrinol. Metab.* **298:** E909–E919.
41. Hayes, M. R., B. C. De Jonghe, and S. E. Kanoski. 2010. Role of the glucagon-like-peptide-1 receptor in the control of energy balance. *Physiol. Behav.* **100:** 503–510.
42. Boudry, G., E. S. David, V. Douard, I. M. Monteiro, I. Le Huërou-Luron, and R. P. Ferraris. 2010. Role of intestinal transporters in neonatal nutrition: carbohydrates, proteins, lipids, minerals, and vitamins. *J. Pediatr. Gastroenterol. Nutr.* **51:** 380–401.
43. Hussain, M. M., P. Rava, X. Pan, K. Dai, S. K. Dougan, J. Iqbal, F. Lazare, and I. Khatun. 2008. Microsomal triglyceride transfer protein in plasma and cellular lipid metabolism. *Curr. Opin. Lipidol.* **19:** 277–284.
44. Gallagher, J. W., R. B. Weinberg, and G. S. Shelness. 2004. ApoA-IV tagged with the ER retention signal KDEL perturbs the intracellular trafficking and secretion of apoB. *J. Lipid Res.* **45:** 1826–1834.
45. Ledford, A. S., R. B. Weinberg, V. R. Cook, R. Hantgen, and G. S. Shelness. 2006. Self-association and lipid binding properties of the lipoprotein initiating domain of apolipoprotein B. *J. Biol. Chem.* **281:** 8871–8876.
46. Ledford, A. S., V. R. Cook, G. S. Shelness, and R. B. Weinberg. 2009. Structural and dynamic interfacial properties of the lipoprotein initiating domain of apolipoprotein B. *J. Lipid Res.* **50:** 108–115.
47. Black, D. D. 2007. Development and physiological regulation of intestinal lipid absorption. I. Development of intestinal lipid absorption: cellular events in chylomicron assembly and secretion. *Am. J. Physiol. Gastrointest. Liver Physiol.* **293:** G519–G524.
48. Antes, T. J., S. A. Goodart, W. Chen, and B. Levy-Wilson. 2001. Human apolipoprotein B gene intestinal control region. *Biochemistry.* **40:** 6720–6730.
49. Yen, C. L., S. J. Stone, S. Koliwad, C. Harris, and R. V. Farese, Jr. 2008. Thematic review series: glycerolipids. DGAT enzymes and triacylglycerol biosynthesis. *J. Lipid Res.* **49:** 2283–2301.
50. Glatzle, J., N. Darcel, A. J. Rechs, T. J. Kalogeris, P. Tso, and H. E. Raybould. 2004. Apolipoprotein A-IV stimulates duodenal vagal afferent activity to inhibit gastric motility via a CCK1 pathway. *Am. J. Physiol. Regul. Integr. Comp. Physiol.* **287:** R354–R359.
51. Whited, K. L., D. Lu, P. Tso, K. C. Kent Lloyd, and H. E. Raybould. 2005. Apolipoprotein A-IV is involved in detection of lipid in the rat intestine. *J. Physiol.* **569:** 949–958.
52. Rubin, D. C., E. A. Swietlicki, J. L. Wang, B. D. Dodson, and M. S. Levin. 1996. Enterocyte gene expression in intestinal adaptation: evidence for a specific cellular response. *Am. J. Physiol.* **270:** G143–G152.